Chinese Chemical Letters 34 (2023) 107921

Contents lists available at ScienceDirect

Chinese Chemical Letters

journal homepage: www.elsevier.com/locate/cclet

Tunable aggregation-induced fluorescent and pressure-responsive luminescence supramolecular cages achieved by subcomponent self-assembly

Lingling Miao[a,1], Xinju Zhu[a,1], Guoxing Liu[c,1], Xin Han[a], Wenping Xie[a], Shuai Lu[d], Long Zhang[b], Kai Wang[b], Linlin Shi[a,*], Siyu Lu[a], Xinqi Hao[a,*], Maoping Song[a,*]

[a] College of Chemistry, Zhengzhou University, Zhengzhou 450001, China
[b] State Key Laboratory of Superhard Materials, College of Physics, Jilin University, Changchun 130012, China
[c] College of Science, Henan Agricultural University, Zhengzhou 450002, China
[d] College of Chemistry and Environmental Engineering, Shenzhen University, Shenzhen 518060, China

ARTICLE INFO

Article history:
Received 29 June 2022
Revised 11 October 2022
Accepted 18 October 2022
Available online 20 October 2022

Keywords:
Supramolecular cage
Self-assembly
Aggregation-induced emission
Solvatochromic fluorescent behavior
Anti-counterfeiting

ABSTRACT

Three discrete tetrahedral metallo-supramolecular cages were designed and constructed using truxene-pended base ligands. Owing to the synergistic rigidifying effect of unsymmetric cyano-substituted oligo(*p*-phenylene-vinylene) (*u*-COPV) suspended by the truxene skeleton, the resulting supramolecular cages were confirmed to exhibit significant aggregation-induced emission (AIE) accompanied by an interesting solvatochromic fluorescent behavior as well as a porous honeycomb-like state during aggregation. In particular, the anti-counterfeiting performance and emission behaviors of the cages in the solid state under external hydrostatic pressure were investigated.

Supramolecular chemistry is the chemistry that achieves the combination of molecules through non-covalent interaction and multiple synergies to obtain the molecular aggregates with ordered structure and specific functions or properties [1,2]. Purposeful selection of suitable angularity, directionality, and stoichiometry of the precursors can be used to construct discrete supramolecular cages with definite cavity structure and size [3–6]. In this regard, subcomponent self-assembly has attracted significant attention as the most powerful bottom-up strategy for the preparation of highly organized structures with diverse functionalities in an "order-out-of-chaos" and a well-controlled manner [7–10]. Meanwhile, the elucidation of structure-property relationships between rigid nanospheres and its pended fluorescent or phosphorescent matrixes facilitates investigations, targeting unique photophysical properties and subsequently benefiting its wide applications in various fields [11,12]. The design and synthesis of novel multi-dimensional structures have always been the main theme of supramolecular research not only because of such interesting structures, but also as a result of a wide range of applications in various fields, including catalysis [13,14], molecular recognition [15–17], biological imitation [18–20], guest sequestration [21–22], drug delivery [23], and membrane transportation [24,25], *etc.*

The non-radiative decay of luminescent molecules is well known to occur because of the geometric distortion of the chromophore, which always competes with fluorescent or phosphorescent efficiency. Since the establishment of aggregation-induced emission (AIE) by Tang and coworkers in 2001, various luminescent systems have been established, which have rendered a far-reaching effect on the development of bioimaging and biosensing and organic optoelectronic materials, *etc.* [26,27]. Compared to traditional luminogens that exhibit marginal or no luminescence in solutions due to active intramolecular motion, molecules with AIE properties exhibit a superior luminous ability in the aggregated state due to the restriction of the intramolecular motion (RIM) mechanism [28–31]. Pressure induced materials under the action of external force, fluorescence produce clear change of materials, heating, recrystallization or solvent method such as fumigation reversible recovery to the initial state of light, this materials in pressure sensor, information storage display, pressure sensor and other fields has a broad application prospect of wide application [32,33].

* Corresponding authors.
E-mail addresses: linlinshi@zzu.edu.cn (L. Shi), xqhao@zzu.edu.cn (X. Hao), mpsong@zzu.edu.cn (M. Song).
[1] These authors contributed equally to this work.

https://doi.org/10.1016/j.cclet.2022.107921
1001-8417/

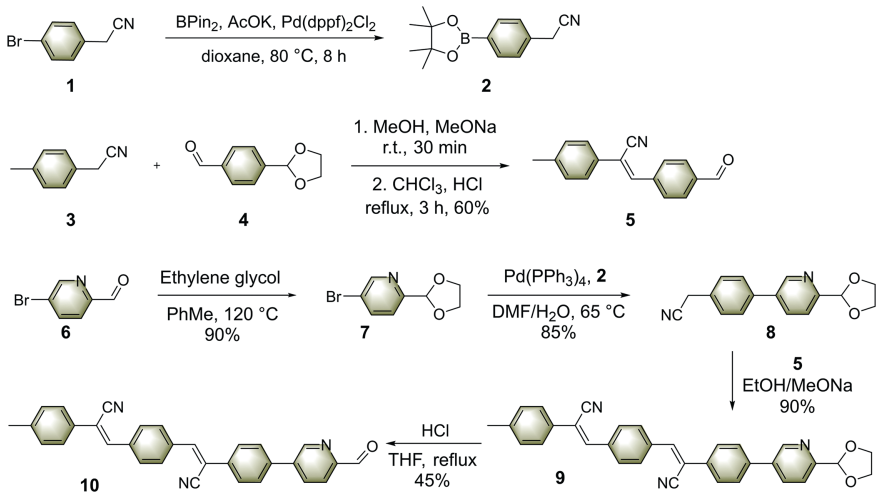

Scheme 1. Synthesis of unsymmetric cyano-substituted oligo(*p*-phenylene-vinylene).

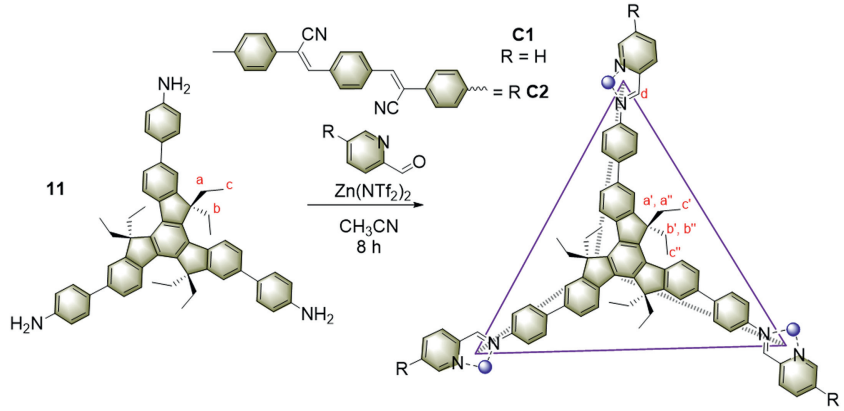

Scheme 2. Synthesis of supramolecule cages **C1** and **C2**.

At present, most of the supramolecular cages with aggregation-induced luminescence effect come from ligands with aggregation-induced luminescence such as tetraphenylethylene, and most of them have hexahedral [34], quadrangular prism [35,36] or planar structures [37], which are beneficial to their stacking in the aggregated state. Truxene is a seven-ring polyaromatic structure with applications in the fields of synthesis, photoluminescence and organic electronics [38–41]. In this paper, trimeric indene with aggregation-induced emission enhancement (AIEE) was used to prepare tetrahedral-type supramolecular cages with aggregation-induced emission, and two tetrahedral-type aggregation-induced emission supramolecular cages were obtained by adjusting the ligands.

Scheme 1 shows the facile preparation of suspended unsymmetric cyano-substituted oligo(*p*-phenylenevinylene) *u*-COPV by convergent synthetic steps. Our synthesis aimed to efficiently construct the key suspended moiety **10**, which carries the required pyridyl aldehyde moiety on its skeleton. Borate ester **2**, which could be easily obtained by the Suzuki coupling reaction with 4-bromobenzeneacetonitrile and bis(pinacolato)diboron, was obtained in an excellent yield, and benzilic aldehyde **5** was generated in a 60% yield by the reaction of **3** and **4**, followed by hydrolysis with dilute hydrochloric acid. Next, the sequential protection and Suzuki coupling transformation of **6** afforded compounds **7** and **8** in 90% and 85% yields, respectively. Finally, the condensation and deprotection of **8** with pre-synthesized **5** afforded the corresponding dissymmetric cyano-substituted oligo(*p*-phenylene-vinylene) **10** in a 45% yield. All building blocks were obtained according to standard synthetic procedures and completely characterized (Figs. S1–S15 in Supporting information).

With the *u*-COPV ligand in hand, the self-assembly of truxene-based amine **11** (1.0 equiv.), pyridyl aldehyde (3.2 equiv.), and zinc bis(trifluoromethylsulfonyl)imide (1.0 equiv.) was accomplished in acetonitrile at room temperature for 8 h, affording desired tetrahedral cage **C1** as a yellow solid in a medium yield. Notably, the self-assembly of cage **C2** was conducted at 70 °C for 8 h to increase the solubility of **10** in acetonitrile (Scheme 2 and Figs. S16–S21 in Supporting information).

To further support the formation of tetrahedral structures, NMR spectroscopy was also employed to obtain structural information about the self-assembled products. Compared with truxene-based amine **11**, cage **C1** exhibited 10 sets of aromatic protons, corresponding to the pyridine and benzene moieties of the structure (Fig. 1a). NMR signals of cage **C2** were observed as clusters of peaks, suggesting that the tetrahedral cage exists as a mixture of diastereomers in solution, in contrast to the other cages prepared by subcomponent self-assembly (Fig. 1c) [42,43]. In addition, significant upfield shifts (1.0–1.2 ppm) of the methylene and methyl moieties compared with that on the free ligand indicated that the ethyl group extends into the cavity after the assembly of tetrahedral cages (Fig. 1b).

Electrospray ionization mass spectrometry (ESI-MS) data demonstrated that cages **C1** and **C2** are substantially stable in solution (Figs. S22 and S23 in Supporting information). As shown

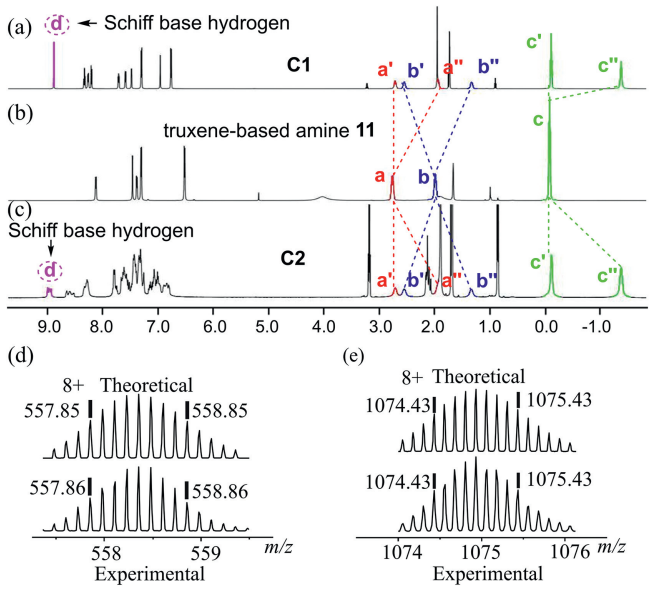

Fig. 1. ^{1}H NMR (600 MHz, CD_3CN, 298 K) spectra of **C1** (a), **11** (b) and **C2** (c). ESI-MS spectra of **C1** (d) and **C2** (e).

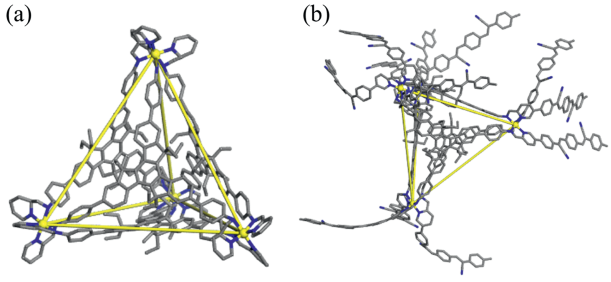

Fig. 2. Energy-minimized molecular model of cage **C2** (Zn, yellow; N, blue; C, gray). Hydrogen atoms and counter anions are omitted for clarity (a) side view hiding the branched chain and (b) top view.

in Figs. S22 and S23, the ESI-MS of cage **C1** revealed one dominant set of peaks with continuous charge states ranging from 5^+ to 8^+ due to the successive loss of (trifluoromethyl-sulfonyl)imide anions (Fig. 1d). Experimental isotope patterns for each peak matched well with simulated isotope patterns, indicative of the formation of a supramolecular ensemble with the proposed stoichiometry (Fig. 1e). After deconvolution, the average molar masses of self-assembled cages **C1** and **C2** were 6697 and 10,827 Da, respectively, matching well with their expected chemical compositions $[(C_{75}H_{66}N_6)_4Zn_4(NTf_2)_8]$ and $[(C_{150}H_{114}N_{12})_4Zn_4(NTf_2)_8]$. Experimental data rules out the possibilities of forming other undesired complexes and isomers. The 2D DOSY spectrum revealed that cage **C1** and cage **C2** are single products, with corresponding diffusion coefficients of 3.26×10^{-10} m^2/s and $8.57 \times 10^{-10} m^2/s$.

A number of efforts focused on gathering complete data of single-crystal X-ray analysis have been unsuccessful; hence, a simulated molecular model of cage **C2** is constructed (Fig. S44 in Supporting information). The simulated molecular model analysis revealed that the supramolecular cage structure of **C2** perfectly matches the designed tetrahedron-like architecture, where truxene units, *u*-COPV moieties, and Zn(II) centers comprise the faces, extended "tails", and vertices, respectively (Fig. 2). Half of the ethyl chains of the truxene moieties pointed into the cavity, while the rest of the faces pointed outwards. The distance between two adjacent Zn(II) centers in the tetrahedron was 24.2 Å, as measured by Materials Studio software.

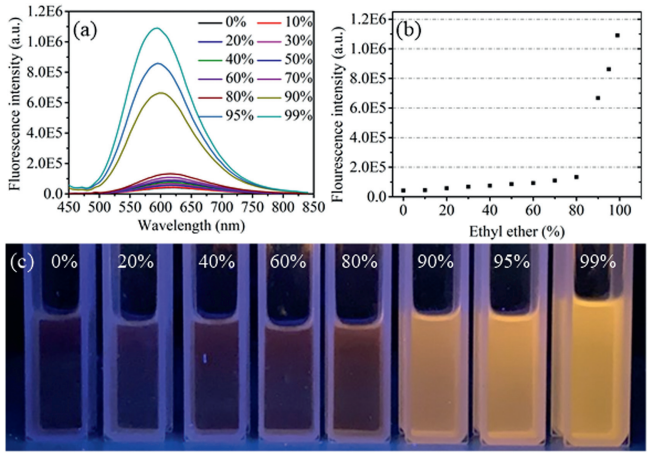

Fig. 3. (a) Emission spectra ($c = 1.0$ μmol/L, $\lambda_{ex} = 430$ nm), (b) changes of emission intensity and (c) fluorescence photographs (5 μmol/L) of **C1** in mixtures of CH_3CN/Et_2O with different f_e.

Supramolecular cages exhibited absorption bands similar to those observed for ligands, and supramolecular cages exhibited red-shifted lower-energy absorption bands compared with those of their constituent ligands (Fig. S25 in Supporting information). This result may be attributed to the coordination of the metal with nitrogen atoms and perturbing the electronic structure of the ligand [44]. Notably, the red-shift degree of the absorption band of cage **C2** was clearly greater than that of **C1**. Therefore, the electronic density of dissymmetric *u*-COPV and π-back bonding from the Zn(II) center to nitrogen π^* is conjectured to enrich the ligand π-system and lower the energy required for excitation. Solvent polarity marginally affected absorption spectra of amine **11**, while solvent polarity exhibited a clear effect on the assemblies (Fig. S26 in Supporting information). Cage **C1** exhibited orange fluorescence in a low-polarity solvent such as acetone, and DMSO led to green emission in conjunction with the blue-shift of the emission band. Solvent polarity has a greater effect on *u*-COPV groups with a greater degree of conjugate, resulting in a supramolecular cage **C2** showing more solvent discoloration effects in different solvents (Figs. S27-S33 in Supporting information).

To further investigate AIE properties of these supramolecular compounds, fluorescence behavior was examined in a mixture of acetonitrile and diethyl ether with different diethyl ether fractions (f_e). According to the results, **C1** exhibited almost no fluorescence as discrete molecules in a good solvent, such as acetonitrile, but **C1** exhibited high luminescence with the increase in f_e from 0% to 99% (Fig. 3). SEM images can also prove that the supramolecular cage **C1** has an obvious aggregation state in f_e from 0% to 99% (Fig. S41 in Supporting information). The fluorescence emission intensity increased nearly 10 times, mainly attributed to the RIM mechanism, which in turn suppresses non radiative relaxation and actuates the energy released through a radiative pathway [45,46].

With the gradual addition of diethyl ether into the solution of cage **C2** in acetonitrile, the emission intensity increased considerably (Fig. 4). With the degree of aggregation increases the distorted molecules tend to be closer to the plane, leading to the red shift of the fluorescence spectrum [47–49]. In other solvent systems, such as dichloromethane/diethyl ether and tetrahydrofuran/diethyl ether, cage **C2** also exhibited an excellent AIE performance with a clear color change (Figs. S34-S37 in Supporting information). Notably, due to the conjugation of *u*-COPV, there may be multiple supramolecular branches stacked during the aggregation process, the electron microscopy images of cage **C2** revealed an interest-

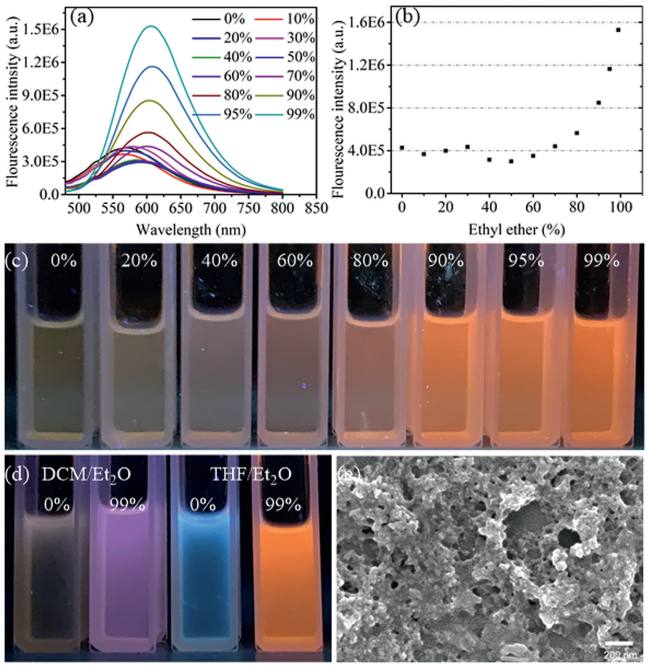

Fig. 4. (a) Emission spectra ($c = 1.0$ μmol/L, $\lambda_{ex} = 450$ nm), (b) changes of emission intensity and (c) fluorescence photographs (5 μmol/L) of **C2** in mixtures of CH_3CN/Et_2O with different f_e. (d) Fluorescence photographs of **C2** (5.0 μmol/L) in mixtures of DCM/Et_2O and THF/Et_2O. (e) SEM photographs of **C2** in CH_3CN/Et_2O mixture with f_e of 99%.

ing porous honeycomb-like structure during aggregation (Fig. S42 in Supporting information) [50,51].

To further explore the suitability of optical properties and provide in-depth explanation on a possible new phenomenon based on the modified metal-organic tetrahedral cage (Fig. 5), a phenylpyridine-ethylene-tailored supramolecular cage **C3** was also synthesized and characterized to systematically explore its AIE behavior (Figs. 5a and b, Figs. S21, S24 and S38 in Supporting information). After experimental exploration, cage **C3** did not exhibit a similar AIE fluorescent behavior in a mixture of acetonitrile and

Fig. 6. Information encryption using cages **C1** and **C2** as the inks.

diethyl ether with different diethyl ether fractions (f_e) compared to cage **C2**. Therefore, the typical AIE and solvatochromic fluorescent properties of cage **C2** may be closely related to the functionalized *u*-COPV structure. The related results revealed that tetrahedral supramolecular cages exhibit clear fluorescence quenching in acetonitrile, and this dark emission fluorescence cannot be lit up by the gradual addition of diethyl ether, and even in a water system.

In addition, whether the emission of two cages would respond to external hydrostatic pressure in the solid state was examined (Figs. 5c and d). The photomicrograph and spectra in the solid state were collected under varying hydrostatic pressure conditions (Figs. S39 and S40 in Supporting information). Both **C1** and **C2** have a red shift of 30 or 40 nm under hydrostatic pressure, mainly due to the pressure induced closer stacking of adjacent molecules and enhanced intermolecular interaction. The *u*-COPV branch of **C2** tends to be flattened under pressure, and the intramolecular charge transfer is enhanced, resulting in greater fluorescence red-shift of **C2** [52]. Meanwhile, the emission intensities of cage **C1** and cage **C2** decreased with the increase in pressure. By the gradually withdrawal of pressure, the fluorescence of cages **C1** and **C2** was recovered to an intermediate level, and the corresponding emission wavelength was blue-shifted to the initial state. Finally, the anti-counterfeiting performance of the cages was also investigated. As the results shown, the "B, e, v, e" in Fig. 6 disappeared with the solution infiltration, while this word reappeared in our field of vision with gradual solvent evaporation (Fig. S43 in Supporting information).

In summary, two tetrahedral metallo-supramolecular cages **C1** and **C2** were prepared by using zinc(II) with truxene-based amine

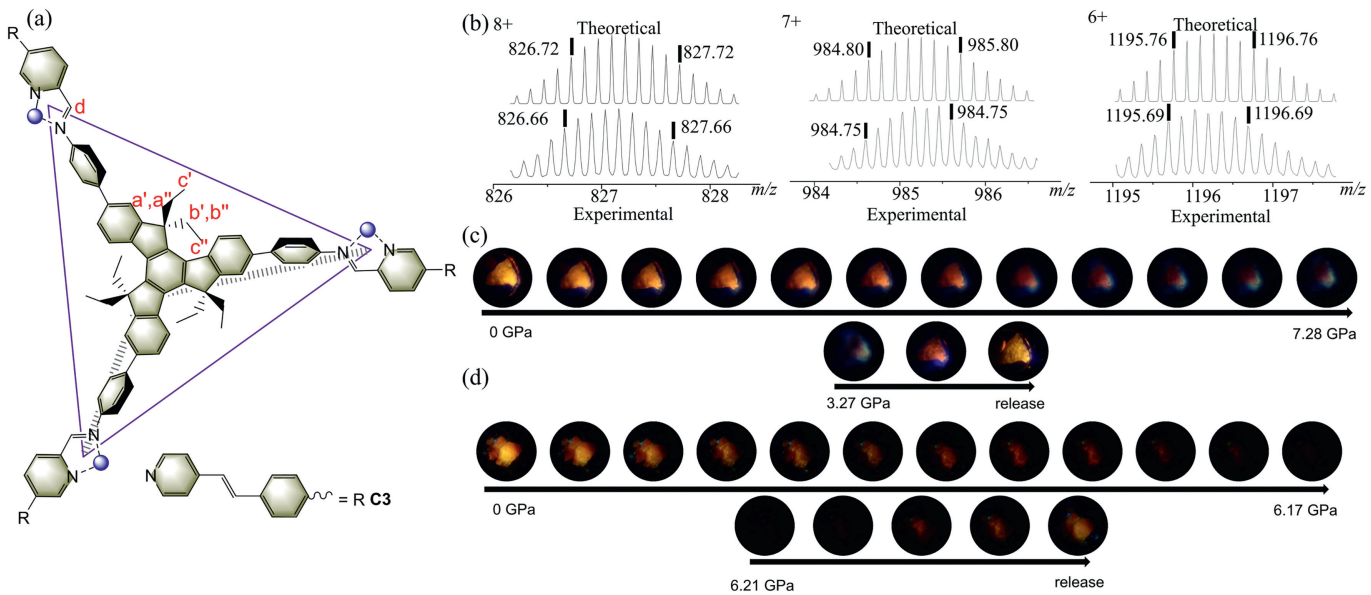

Fig. 5. (a) Structure of supramolecular **C3**. (b) Presentive ESI-MS spectra of **C3**. Fluorescence emission responses by the gradual withdrawal of photographs of **C1** (solid) (c) and **C2** (solid) (d).

and *u*-COPV, followed by detailed NMR and mass spectrometry characterization. Owing to the tunable fluorescence rendered by *u*-COPV and truxene-based amine, the cage assemblies were confirmed to exhibit significant AIE, accompanied by an interesting solvatochromic fluorescent behavior and porous honeycomb-like structures during aggregation. Furthermore, emission behaviors of the cages in the solid state under external hydrostatic pressure were investigated. More specifically, stimuli-responsive results and anti-counterfeiting performance endowed high potential to these supramolecular cages for the development of high-performance fluorescent materials with tailored functionality.

Declaration of competing interest

The authors declare that they have no known competing financial interests or personal relationships that could have appeared to influence the work reported in this paper.

Acknowledgments

We thank the National Natural Science Foundation of China (Nos. 22101267, 21672192, 21803059, U2004191, U1904212, 21801063) for financial support. We also acknowledge the Molecular Scale Laboratory (Shenzhen University) for mass spectrometry characterization.

References

[1] J.M. Lehn, Pure Appl. Chem. 50 (1978) 871–892.
[2] J.M. Lehn, Science 260 (1993) 1762–1763.
[3] X. Yan, T.R. Cook, P. Wang, et al., Nat. Chem. 7 (2015) 342–348.
[4] M.L. Saha, X. Yan, P.J. Stang, Acc. Chem. Res. 49 (2016) 2527–2539.
[5] T. Feng, X. Li, J. Wu, et al., Chin. Chem. Lett. 31 (2020) 95–98.
[6] Z. Zhang, Z. Zhao, L. Wu, et al., J. Am. Chem. Soc. 142 (2020) 2592–2600.
[7] G.M. Whitesides, B.S. Grzybowski, Science 295 (2002) 2418–2421.
[8] S. Leininger, B. Olenyuk, P.J. Stang, Chem. Rev. 100 (2000) 853–908.
[9] R. Chakrabarty, P.S. Mukherjee, P.J. Stang, Chem. Rev. 111 (2011) 6810–6918.
[10] A. Kumar, E. Zangrando, S.K. Jewrajka, Polyhedron 172 (2019) 67–73.
[11] A. Svendsen, H.V. Kiefer, H.B. Pedersen, et al., J. Am. Chem. Soc. 139 (2011) 8766–8771.
[12] K.Z. Su, S.F. Du, W.J. Wang, et al., Chin. Chem. Lett. 31 (2020) 2023–2026.
[13] W. Cullen, M.C. Misuraca, C.A. Hunter, et al., Nat. Chem. 8 (2016) 231–236.
[14] W. Cullen, H. Takezawa, M. Fujita, Angew. Chem. Int. Ed. 58 (2019) 9171–9173.
[15] R.J. Li, J.J. Holstein, W.G. Hiller, et al., J. Am. Chem. Soc. 141 (2019) 2097–2103.
[16] S. Oldknow, D.R. Martir, V.E. Pritchard, et al., Chem. Sci. 9 (2018) 8150–8159.
[17] M.J. Burke, G.S. Nichol, P.J. Lusby, J. Am. Chem. Soc. 138 (2016) 9308–9315.
[18] M.J. Wiester, P.A. Ulmann, C.A. Mirkin, Angew. Chem. Int. Ed. 50 (2011) 114–137.
[19] M. Mondal, A.K.H. Hirsch, Chem. Soc. Rev. 44 (2015) 2455–2488.
[20] D. Zamora-Olivares, T.S. Kaoud, K.N. Dalby, et al., J. Am. Chem. Soc. 135 (2013) 14814–14820.
[21] C. García-Simón, M. Garcia-Borràs, L. Gómez, et al., Nat. Commun. 5 (2014) 5557.
[22] Y.L. Lai, H.J. Zhang, J. Su, et al., Chin. Chem. Lett. (2022), doi:10.1016/j.cclet.2022.07.029.
[23] T. Sawada, M. Yoshizawa, S. Sato, et al., Nat. Chem. 1 (2009) 53–56.
[24] S.K. Samanta, D. Moncelet, V. Briken, et al., J. Am. Chem. Soc. 138 (2016) 14488–14496.
[25] S.K. Samanta, J. Quigley, B. Vinciguerra, et al., J. Am. Chem. Soc. 139 (2011) 9066–9074.
[26] Y.Y. Liu, X. Zhang, K. Li, Angew. Chem. Int. Ed. 60 (2021) 22411–22423.
[27] Q. Peng, Y. Yi, Z. Shuai, et al., J. Am. Chem. Soc. 129 (2007) 9333.
[28] J.B. Xiong, H.T. Feng, J.P. Sun, et al., J. Am. Chem. Soc. 138 (2006) 11469–11472.
[29] M. Zhang, M.L. Saha, M. Wang, et al., J. Am. Chem. Soc. 139 (2011) 5067–5074.
[30] Y. Hong, J.W.Y. Lam, B.Z. Tang, Chem. Soc. Rev. 40 (2011) 5361–5388.
[31] T. X.Xiao, J. Wang, Y. Shen, et al., Chin. Chem. Lett. 32 (2021) 1377–1380.
[32] C. Ge, C.Y. Liu, X. Ye, et al., Mater. Chem. Front. 1 (2017) 530–537.
[33] L.D. Dai, Y.K. Zhuang, H.P. Li, et al., Mater. Chem. C 5 (2017) 12157–12162.
[34] X.Z. Yan, M. Wang, T.R. Cook, et al., J. Am. Chem. Soc. 138 (2016) 4580–4588.
[35] X.Z. Yan, T.R. Cook, P. Wang, et al., Nat. Chem. 7 (2015) 342–348.
[36] G.F. Li, Z.X. Zhou, C. Yuan, et al., Angew. Chem. Int. Ed. 59 (2020) 10013–10017.
[37] L.J. Chen, Y.Y. Ren, N.W. Wu, et al., J. Am. Chem. Soc. 137 (2015) 11725–11735.
[38] K.Q. Zhao, C. Chen, H. Monobe, et al., Chem. Commun. 47 (2011) 6290–6292.
[39] H.L. Ni, H. Monobe, P. Hu, et al., Liq. Cryst. 40 (2013) 411–420.
[40] X. Liu, T.U. Sui, J. Hanna, Chem. Mater. 26 (2014) 5437–5440.
[41] F. Goubard, F. Dumur, RSC Adv. 5 (2015) 3521–3551.
[42] W. Meng, J.K. Clegg, J.D. Thoburn, et al., J. Am. Chem. Soc. 133 (2011) 13652–13660.
[43] W. Meng, B. Breiner, K. Rissanen, et al., Angew. Chem. Int. Ed. 50 (2011) 3479–3483.
[44] Z. Li, Y. Han, F. Nie, et al., Angew. Chem. Int. Ed. 60 (2021) 8212–8219.
[45] F. Bu, R.H. Duan, Y.J. Xie, Angew. Chem. Int. Ed. 54 (2015) 14492–14497.
[46] X.L. Peng, S. Ruiz-Barragan, Z.S. Li, Mater. Chem. C 4 (2016) 2802–2810.
[47] Y.J. Wang, Y. Shi, Z.Y. Wang, et al., Chem. Eur. J. 22 (2016) 9748–9791.
[48] Y. Teng, B.W. Wang, S.Q. Cui, et al., Dyes Pigm. 186 (2021) 109029.
[49] M.Q. Yang, J.R. Deng, H.F. Su, et al., Mater. Chem. Front. 5 (2021) 406–417.
[50] H.C. Yeh, W.C. Wu, Y.S. Wen, et al., J. Org. Chem. 69 (2004) 6455–6462.
[51] Y.P. Li, F. Li, H.Y. Zhang, et al., Chem. Commun. (2007) 231–233.
[52] S. Hayashi, Mol. Syst. Des. Eng. 6 (2021) 503–507.